

Study of Structural, Thermic, μ -Raman and Optic Transformation of PVA/TiO₂ Polymeric Membranes

Juan David Romero Salazar

¹Ingeniería física, Universidad Nacional de Colombia-Sede Manizales, Manizales, Colombia

Resumen—Se sinterizaron membranas compuestas (1-x)PVA/xTiO₂ (0,025≤x≤0,250) por mezclas en disolución acuosa. La influencia de los rellenos cerámicos de TiO₂ sobre la matriz polimérica de PVA se estudió por espectroscopía μ -Raman, difracción de rayos-X (XRD), calorimetría diferencial de barrido (DSC), análisis termo-gravimétrico (TGA), absorción UV-visible y microscopía de barrido electrónico (SEM). Resultados Raman y XRD mostraron las fases amorfa y monoclinica para el PVA y la fase anatasa para el TiO₂. Micrografías SEM mostraron los rellenos de TiO₂ dispersos en la matriz polimérica de PVA formando agregados. Resultados DSC y TGA mostraron transiciones de fase con la temperatura, la temperatura de transición vítrea (T_g) y la estabilidad térmica de la matriz polimérica. La energía de band gap óptico (E_g) relacionada con el TiO₂ (anatasa) se calculó de medidas UV-visible, mostrándose una fuerte absorción en la región UV-cercana debido a los rellenos cerámicos.

Palabras clave— Polyvinyl Alcohol, Anatasa, Espectroscopia μ -Raman, XRD, Cristalinidad, Fases térmicas, Band Gap, DSC, TGA.

Abstract— Composites (1-x)PVA/xTiO₂ (0,025≤x≤0,250) were prepared from aqueous solution. The influence of TiO₂ ceramic fillers on polymer matrix was characterized by: X-ray diffraction (XRD), differential scanning calorimetry (DSC), thermogravimetric analysis (TGA), micro-Raman scattering, UV-visible absorption (UV-vis) and scanning electronic microscopy (SEM). Raman and XRD results showed the amorphous and monoclinic phases for PVA and anatase phase for TiO₂. SEM micrographs showed spread TiO₂ fillers in PVA polymeric matrix forming aggregates. DSC and TGA thermograms show phase transitions with temperature, glass transition temperature (T_g) and thermal stability of polymeric matrix. The band gap energy (E_g) related to TiO₂ (anatase) has been calculated from UV-visible measures, showing a strong absorption at near-UV region due to ceramic fillers.

Key Word — Polyvinyl Alcohol, Anatase, μ -Raman Spectroscopy, XRD, Crystallinity, Thermal Phases, Band Gap, DSC, TGA.

I. INTRODUCTION

Polyvinyl alcohol (PVA) is recognized among of few vinyl polymers capable to dissolve in water [1]. Its repetitive unity is

-CH₂-CHOH-, the alcohol group OH- is located on alternating carbon atoms. Due to hydroxyl groups, the PVA is characterized by a strongly hydrophilic nature and forming hydrogen bonding. As most of vinyl polymers, the PVA is not obtained by polymerization of corresponding monomer, but it is produced by partial or complete hydrolysis of polyvinyl acetate removing the acetate groups. The PVA is an atactic material showing crystallinity due to hydroxyl groups which are sufficiently small to adjust in the cell without disrupt it [2]. PVA blends dispose of significant practical utility [3] thanks to their low cost, availability, excellent mechanical strength, biocompatibility and non-toxicity [4]. Main applications of PVA include several materials like paper, textiles, films with resistance to oxygen, adhesives, food wrappers, membranes at desalination and pervaporation [5], cosmetics, pharmacy and electronic industry [1].

Titanium dioxide (TiO₂) is commercially produced since 1923. The bulk material shows three structural phases: anatase, rutile and brookite. TiO₂ exists mostly at anatase and rutile phases, having a tetragonal structure. The rutile is a stable phase at high temperatures and has optical band gap energy of 3,0 eV (415 nm), and anatase is formed at lower temperatures with an optical band gap energy of 3,2 eV (380 nm) [6]. The TiO₂ is used in broad variety of applications and products, such as catalysis, dielectric materials, charge separators devices, chemical sensors, photoconductors, solar cells, microelectronics, electrochemical, and owing to high durability and photo-catalytic activity, low cost, excellent stability under illumination and non-toxic nature, the TiO₂ has an extensive utility on air purification, solar energy conversion, treatment of wastewaters, paints, plastics, inks, paper as white pigment and recovering [6-8].

In order of improving the conductivity and the permeability in water, PVA membranes are treated with solvents or modified with solid fillers [9-11]; for example, ceramic fillers as TiO₂ (PVA/TiO₂ [9-11]), SiO₂ (PVA/SiO₂ [5,11]), and hydroxyapatite (PVA/HAP [2,11]) are employed. Addition of ceramic particles in polymeric matrix has been reported to reduce the glass transition temperature (T_g) and polymer crystallinity, augmenting amorphous phases at polymeric

matrix and then, the ionic conductivity. The increase of ionic conductivity is explicated by the fact that ceramic fillers in polymeric matrix create some defects and free volume at interface between ceramic particles and polymeric chain [9-11].

In this work, the study of effect in concentration changes of TiO₂ ceramic fillers on PVA polymeric matrix will be shown. The results of this survey will be introduced under the following topics; first, changes at crystalline phases due to incorporation of TiO₂ (anatase) fillers at polymeric matrix (Raman spectroscopy and XRD); second, the effect of ceramic fillers and water molecules on thermal phases transitions at PVA (Raman spectroscopy and DSC); third, the thermal stability (DSC and TGA); and fourth, the optical absorption due to TiO₂ incorporation (UV-vis absorption).

II. MATERIALS AND METHODS:

PVA (Merck, hydrolysis degree: 98%, m.w. 60000) and TiO₂ (Sigma-Aldrich, Titanium (IV) oxide, anatase) powders was utilized with no additional purification. PVA/TiO₂ polymeric membranes were synthesized by blends at aqueous dissolution. Appropriated weight PVA: TiO₂ relations (1-x: x, x = 0,025, 0,050, 0,075, 0,100, 0,125, 0,150, 0,200 and 0,250) were kept under magnetic stirring at deionized water. PVA and TiO₂ blends were prepared at 85°C for 1h, but under constant magnetic stirring for 24h until homogeneous solutions at room temperature were obtained, then both solutions were blended at 85°C for 1h, and under constant magnetic stirring by 4h until a viscous and homogeneous blend was gotten. The obtained dissolution was submitted to ultrasound for 1h, allowing degasification and an improved dispersion of TiO₂ particles. The resulting solutions were deposited on Teflon plates and the membranes were dried at 80°C for 16h and then, they were removed. The obtained thickness at polymeric films was between 100 and 150 μm. Crystalline structure of the composites was evaluated using a Rigaku Miniflex2 diffractometer, λ = 1,540562 Å, the XRD patterns were recorded at room temperature for 2θ angles between 5 and 80°, with a scanning rate of 2°/min and steps of 0,02°. Raman analysis were made with a Confocal Raman Labram HR 800 (Horiba Jovin Yvon) system, using a monochromatic laser beam of 473 nm as excitation source. Raman spectra were taken for frequencies from 150 to 3600 cm⁻¹, with heating from 22 to 200°C and steps of 20°C per measure. DSC and TGA thermal analysis were made at rate of 5°C/min in a N₂ atmosphere by heating from -40 to 350°C for DSC, and from 20 to 600°C for TGA, using TA instruments systems (DSC Q100 and TGA Q500). UV-visible spectra were recorded with a Perkin Elmer Lambda 20 UV/vis spectrometer in a range between 350 and 500 nm at room temperature. Membranes morphology was observed with a Scanning Electronic Microscope (Pelco SC7 SEM, Gold Sputtering System, 40 mA, and discharge time 20 s). EXPGUI-GSAS software (2006 version) [12] was employed for refinement of cell parameters of PVA and TiO₂ (anatase) crystalline structures, and background function. Crystallinity,

Full Width at Half Maximum (FWHM) and XRD peak integration were determined using MDI Jade 6.5 software. Preferential orientations were indexed with the reported at Powder Diffraction Files (AMCSD-0010737 and AMCSD-0010738 files, from American Mineralogist Crystal Structure Database, and PDF files No 21-1272 and No 71-1169, from International Centre for Diffraction Data). Raman spectra were fitted using Gaussian profiles with OriginPro8 software and the background was extracted with Fityk 0.8.9 software [13]. The analysis of thermal properties was studied by using TA Universal Analysis software.

III. RESULTS AND DISCUSSION:

A. μ-Raman spectroscopy:

Figures 1-2 show Raman spectra at different temperatures for PVA: TiO₂ polymeric membranes, x=0,05 (Figure 1) and x=0,10 (Figure 2). Characteristic peaks are shown at 1440, 1383, 1146, 917 and 854 cm⁻¹ for PVA, and 145, 194, 398, 517 and 638 cm⁻¹, for stretching and bending vibrations of O-Ti-O and Ti-O groups for anatase. The frequencies of important Raman peaks for PVA and TiO₂ (anatase) are listed in table 1. For purpose of calculus, the band at 1440 cm⁻¹ was taken as reference [18], because it suffers only a slight shift with temperature. The band at 1146 cm⁻¹ is an indicator of crystallinity degree at PVA polymeric matrix [9,18], and the located at 1383 cm⁻¹ is attributed to a coupling of O-H in the plane vibration (strong peak at 1440 cm⁻¹) with C-H wagging vibration [20]. Therefore, intensity relations of peaks (Figures 3(a-b)) were taken as a measure of crystallinity at polymeric matrix (between 1146 and 1440 cm⁻¹), and as a reference of ceramic-polymer interaction (between 1440 and 1383 cm⁻¹).

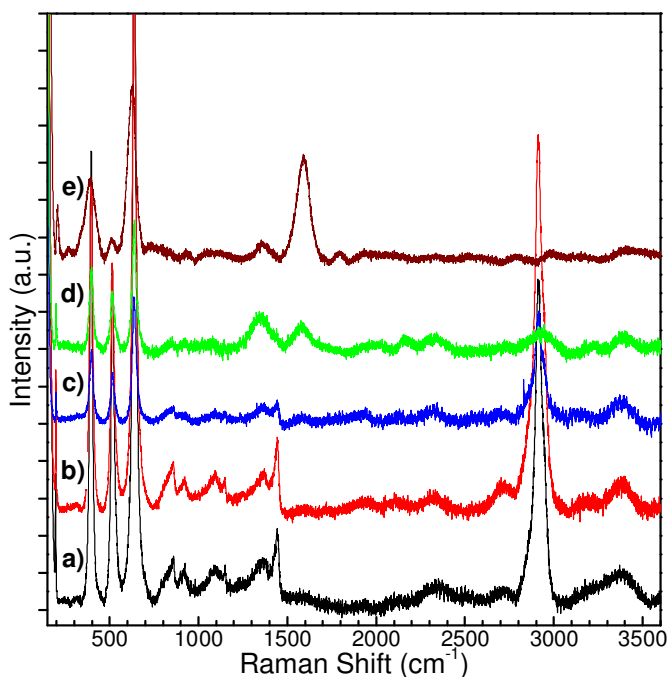


Figure 1. Raman spectra of PVA: TiO₂ composite (x=0,05) at different temperatures; (a) 22, (b) 79, (c) 104, (d) 128 and (e) 184°C.

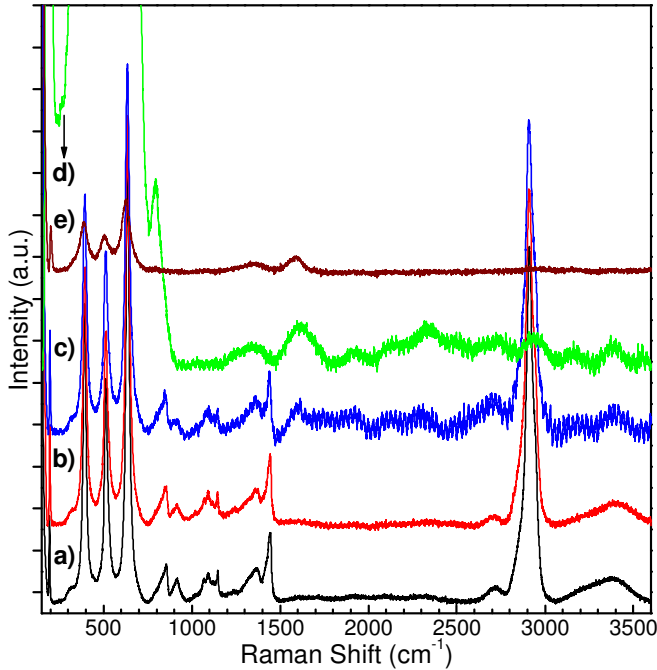


Figure 2. Raman spectra of PVA: TiO₂ composite (x=0,10) at different temperatures; (a) 21, (b) 82, (c) 110, (d) 128 and (e) 199°C.

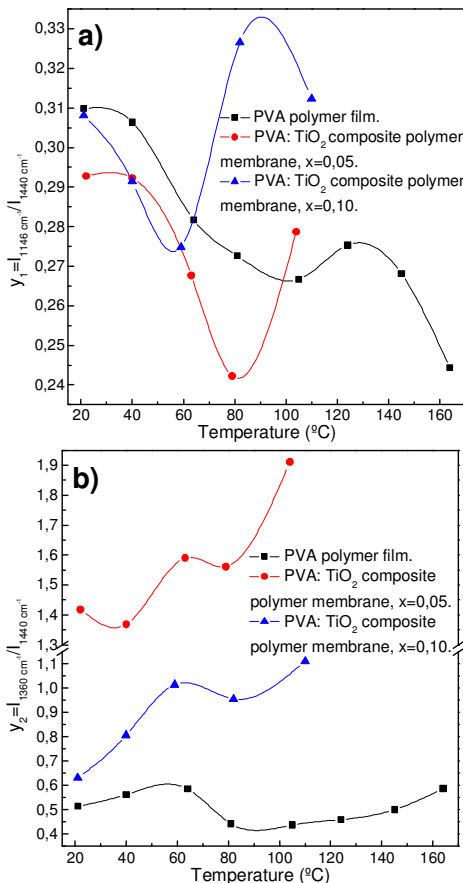


Figure 3. Intensity relations of bands between; (a) 1146 and 1440 cm⁻¹ (y₁), and (b) 1360 and 1440 cm⁻¹ (y₂).

Frequency (cm ⁻¹)	Assignment	References
PVA membrane		
3107–3495	–OH stretching	[14–17]
2870–2942	CH ₂ stretching	[14–18]
1440	O–H bending, CH ₂ symmetric bending.	[9,11,17]
1383	C–H and O–H bending	[9]
1258	C–C and C–O stretching	[11]
1146	C–O and C–C stretching. Crystallinity.	[9,11,17]
1093	C–O stretching, O–H bending	[9,11]
917	C–C stretching	[9]
916	CH ₂ rocking	[18]
854	C–C and CH ₂ stretching	[9]
850	C–C–O stretching	[18]
TiO ₂ anatase powders		
145	O–Ti–O bending (E _g)	[9,19]
194	O–Ti–O bending (E _g)	[9,19]
398	O–Ti–O bending (B _{1g})	[9,19]
517	Ti–O axial stretch vibration (A _{1g} + B _{1g})	[9,19]
638	Ti–O equatorial stretch vibration (E _g)	[9,19]

Table 1. Raman characteristic bands of PVA and TiO₂ (anatase).

The calculated relations (Figures 3(a-b)) show vibrational phases at PVA. This calculation present two pronounced tendencies in function of temperature; the first between 40 and 85°C indicates the glass transition, whereby non-freezable bound water molecules [5,21] act as plasticizers, and the second from 85 to 110°C is characterized for release superficial water (i.e. water non-bounded through hydrogen bonding [5]) in the macromolecular structure, also related to thermal history of polymer during the synthesis, annealing and crystallization of membranes [22]. Figures 3(a-b) exhibit other thermal phase at PVA polymeric membrane between 120 and 160°C, which is characterized by β-relaxation of crystalline phases [23,24], consisting of augment at molecular mobility of crystals, increasing differently the cell parameters [25], and attaining better crystalline perfection [22,26]. At temperatures above 160°C, fast and directional evaporation of non-freezable bound water molecules is produced [21,26], then the chains and hydroxyl groups of PVA acquire more ordered orientation. Therefore, an augment of fluorescence at Raman spectra is generated with disappearance of low energy vibrational modes associated to PVA, due to molecular conformation change on membrane surface with hydroxyl groups uniformly oriented at water evaporation direction [27].

At PVA/TiO₂ composite membranes, vibrational decoupling due to interaction between TiO₂ fillers and -OH groups of PVA [20] is confirmed with augmentation at intensity relation of bands at 1440 and 1383 cm⁻¹ (Figure 3(b)). Raman spectra at Figures 1-2 show the fluorescence augment at approximated 110°C, low energy vibrational modes of PVA vanishing, and appear of a peak corresponding to band between 1500 and 1700 cm⁻¹. Therefore, a decrease at temperature of molecular conformation change at composite films surface is attributed to ceramic fillers addition, which generates structural

reorientation of amorphous phases at polymeric matrix, and decrease at temperature and energy associated with non-freezable bound water molecules evaporation. Crystallinity at PVA polymeric matrix and TiO₂ (anatase) vibrational modes are also sensitives at thermal vibrational phases of PVA: TiO₂ composite (Figures 1-3).

B. X-ray diffraction (XRD):

It is frequently said that PVA molecules are disposed in a zigzag conformation with a step per monomer of 2,52 Å. In 1948, Bunn [28] suggested a crystalline structure for PVA containing a random distribution of syndiotactic and isotactic units. The structure has two polymer molecules disposed through each unit cell. Each repetitive monomer contains two hydroxyl sites, each one with an occupation of 50%, then creating an atactic structure. The cell is monoclinic ($a = 7,81$ Å, $b = 2,52$ Å (chain axis), $c = 5,51$ Å, $\alpha = \gamma = 90^\circ$, $\beta = 91,7^\circ$) [18,25,28,29], and with a symmetry corresponding to spatial group P2₁/m [28]. Anatase has a tetragonal crystalline structure. The symmetry of unit cell corresponds to spatial group D_{4h} (I4₁/amd) containing two formula units. The cell parameters are taken as $a = 3,785$ Å and $c = 9,514$ Å, and the structure is octahedral coordinated [19,30,31].

For this case, X-ray patterns of PVA polymeric film and TiO₂ (anatase) powders are shown at Figure.4(i), and PVA: TiO₂ composite membranes at Figure.4(ii). The patterns are evidenced as Bragg reflections associated to PVA monoclinic planes at 2θ around 11,3 (100), 18,8 (10 $\bar{1}$), 19,3 (101), 22,8 (200), 27,2 (20 $\bar{1}$), 27,9 (201), 38,0 (20 $\bar{2}$), 39,0 (202), 40,6 (11 $\bar{1}$) and 40,9° (111) [25,32-34], another associated with planes (110), (30 $\bar{1}$), (301) and (001) and a last group associated to reflections (102), (10 $\bar{2}$) and (300); this two former groups were calculated with EXPGUI-GSAS software [12] at ranges from 38,0 to 42,0 and between 33,0 and 36,0° respectively, and they were also obtained by Cho et al. [29] and Assender et al. [34] using molecular dynamics for chains with different stereoregularities. Tetragonal planes of anatase phase (JCPDS cards No 21-1272 and 71-1169 [35]) have been evidenced with reflections around 25 (101), 37 (103), 38 (004), 48 (200), 54 (105), 55 (211), 62 (213), 63 (204), 69 (116), 70 (220) and 75° (215).

Figure 5 shows relative intensities calculated with representative peaks for PVA and TiO₂. For 100x values in the interval from 2,5 to 7,5, ceramic fillers destroy notably crystalline phases of PVA, so that the fall at intensity relation presents a strong decrease, this tendency for 100x higher to 7,5 is relaxed and stabilized at values next to zero. For TiO₂ high concentrations (100x>7,5), instead of destroying crystalline phases of PVA, ceramic fillers rather augment the free space [9-11] and change non-freezable bound water molecules orientation in the polymeric matrix, stimulating the short-range order at amorphous phases [26] and keeping crystalline regions intact. Changes at a and c parameters of PVA monoclinic cell (Table 2) were sensitives to decrease of crystalline phases; for

100x between 2,5 and 7,5, cell parameters change notably, but for 100x values higher to 7,5, they approach again to reference parameters [18,25,28,29]; the distance between repetitive unities (b parameter) at zig-zag conformation of polymeric chains was maintained unchanged [36]. For 100x values less than 15,0, TiO₂ cell parameters (Table 3) approach to references [19,30,31,35] without exhibit some special tendency. Then, it is concluded that PVA and TiO₂ crystalline phases are independent, and ceramic fillers are accommodated in the amorphous phase of PVA.

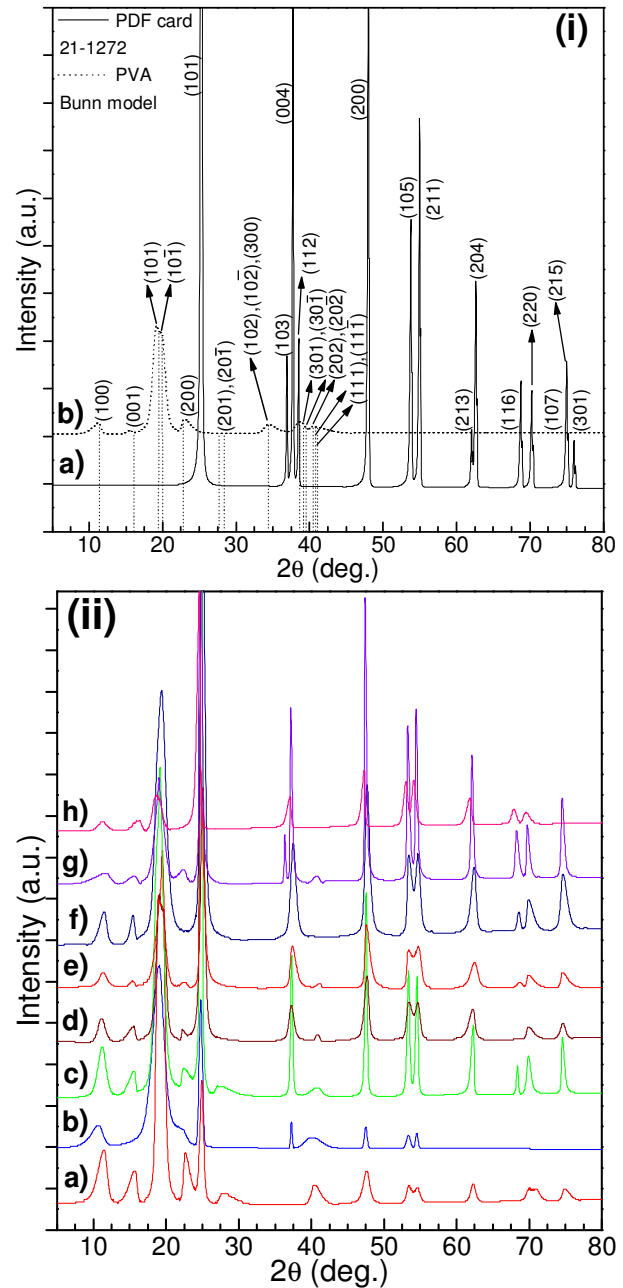


Figure 4.(i) XRD patterns of; (a) TiO₂ (anatase) powders and (b) PVA polymer film. (ii) XRD patterns of PVA: TiO₂ composite membranes, x equal to; (a) 0,025, (b) 0,050, (c) 0,075, (d) 0,100, (e) 0,125, (f) 0,150, (g) 0,200 and (h) 0,250.

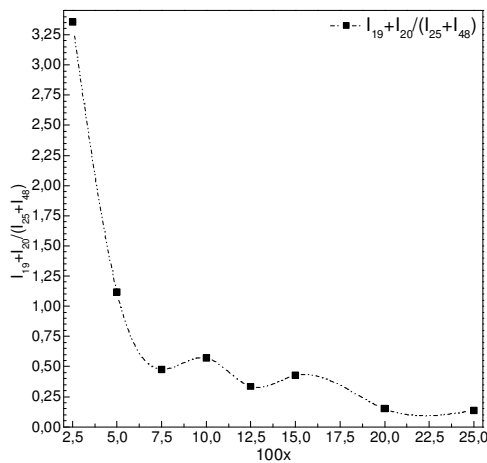


Figure 5. Intensities relation calculated using references peaks for PVA (2θ around 18,8 and 19,3) and TiO_2 (around 25,0 and 48,0°).

100x	a (Å)	c (Å)
2,5	7,8252±0,0070	5,6934±0,0098
7,5	7,7958±0,0048	5,5697±0,0073
10,0	7,7842±0,0011	5,5269±0,0009
12,5	7,7925±0,0014	5,5200±0,0009
15,0	7,7937±0,0009	5,5232±0,0006
20,0	7,7959±0,0015	5,5487±0,0017
25,0	7,7860±0,0054	5,5034±0,0039
PVA polymer film	7,7976±0,0086	5,5027±0,0071

Table 2: Lattice parameters for PVA

100x	a (Å)	c (Å)
2,5	3,7942±0,0046	9,5688±0,0296
7,5	3,8061±0,0007	9,5467±0,0031
10,0	3,8023±0,0004	9,6251±0,0089
12,5	3,8006±0,0004	9,5546±0,0046
15,0	3,7998±0,0003	9,5838±0,0068
20,0	3,8993±0,0011	9,5002±0,0025
25,0	3,8349±0,0021	9,6578±0,0058
TiO_2 powders	3,7881±0,0006	9,5213±0,0017

Table 3. Lattice parameters for TiO_2

Table 4 shows crystalline sizes estimated through different methods for TiO_2 anatase phase. The deviation of cell

100x	Crystallite size (nm) ¹	Strain (%) ¹	Crystallite size (nm)		
			D ₁ ¹	D ₂ ³	D ₃ ²
2,5	22,1±1,7	0,424±0,043	12,9±0,2	14,2±0,4	13,4±1,0
7,5	39,5±1,9	0,122±0,014	27,8±0,3	30,0±1,0	37,2±0,8
10,0	13,7±0,6	0,218±0,040	11,1±0,2	11,0±1,0	12,5±0,6
12,5	17,4±2,4	0,432±0,087	12,0±0,3	13,4±0,7	13,1±0,4
15,0	15,4±0,9	0,165±0,044	12,6±0,2	13,0±1,0	13,2±0,3
20,0	40,5±3,4	0,105±0,021	28,4±0,6	32,0±2,0	39,5±1,0
25,0	20,2±2,2	0,163±0,063	15,9±0,5	17,0±2,0	21,7±0,6
TiO_2 powders	78,4±5,2	0,020±0,009	68,2±1,4	68,0 ±2,0	73,4±0,6

Table 4. Crystallite size for anatase phase at composite PVA/ TiO_2 membranes.

¹ Stimmed with MDI Jade6.5 software through Williamson–Hall method (D₁ does not take into account micro-deformations).

² D₃ and D₄ were stimmed from Debye–Scherrer equation with EXPGUI-GSAS software, for separated PVA and TiO_2 (anatase) phases, including instrumental correction ($\frac{K\lambda}{D}$ is a constant, D is the crystallite size, and K is taken with a value of 1).

³ Evaluated with MDI Jade6.5 software, with FWHM of reflections at $2\theta \approx 25,0$ (D₂), 11,3 (D₅), 18,8 (D₆) and 19,3° (D₇), using Debye–Scherrer equation and including instrumental correction.

parameters (Table 3) and the less crystallite sizes (Table 4) compared with precursor powder ($a = 3,7881(6)$ Å, $c = 9,5213(17)$ Å, $D \approx 68$ nm) show a polycrystalline growing of TiO_2 with higher disorder degree in the amorphous phase of PVA polymeric matrix, so that strain generated by defects at TiO_2 fillers and interface with polymeric matrix should be considered [9-11]. Division of doublet at 2θ around 53-55° [37] and bigger deformation of cell parameters for smaller crystalline sizes [30] are taken as a measure of crystalline quality for anatase phase (Figure.4(ii)). Table 5 shows crystalline sizes calculated utilizing Scherrer equation from reflections at $2\theta \approx 18,8$ ($10\bar{1}$), 19,3 (101) and 11,3 (100) corresponding to ordered phases of PVA. Crystallite sizes associated with reflections at ($10\bar{1}$) and (101) are higher for PVA: TiO_2 composite system than PVA polymeric film; crystalline size associated with short-range order of amorphous phases at (100) direction is kept between 5–7 nm [26]. The fact mentioned above confirms improving crystals for great x values ($100x > 7,5$) and the strengthening of alignment between neighbor polymeric chains at amorphous regions [26], due to additional formation of free space [9–11] changing molecular conformation of PVA chains and their interaction with water molecules [26]. The instrumental data was taken from XRD pattern of calibration sample (Silicon).

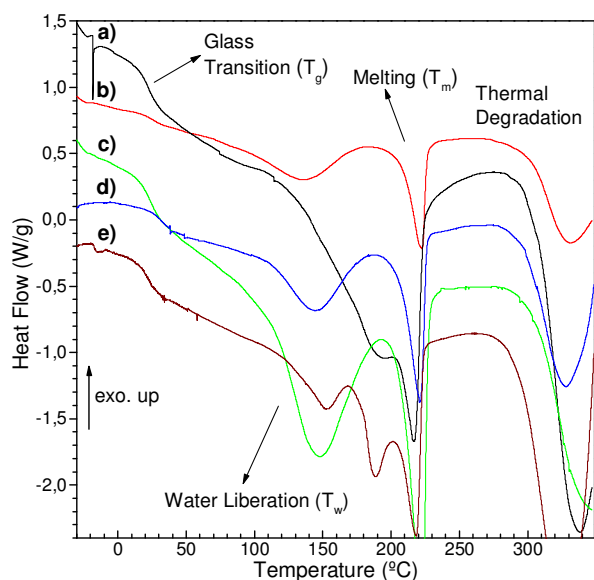
C. Differential Scanning Calorimetry (DSC):

Figure.6 shows DSC thermograms for PVA: TiO_2 composite membranes. The values at glass transition temperature (T_g) are smaller than reported for bulk PVA (approx. 75°C for fully hydrolyzed degree [38]), that is generally because the water molecules become plasticizers augmenting free space in the polymeric matrix [23]. Thermograms also show endothermic phase transitions for PVA: TiO_2 composites associated to non-freezable bound water molecules released from surface, melting of PVA crystalline phase and decomposition of polymeric chain. Table 6 shows values associated with polymer thermal process shown at Fig.6 at PVA: TiO_2 composites membranes; glass transition (T_g) and evaporation of superficial and non-freezable bound water, at amorphous phase; and β -relaxation and melting (T_m), at crystalline phase [5,21-24,39].

100x	Crystallite size (nm)			
	D ₄ ²	D ₅ ³	D ₆ ³	D ₇ ³
2,5	6,9±0,2	5,2±0,3	9,4±1,1	9,2±0,8
7,5	11,3±0,4	6,0±0,3	10,2±1,2	11,3±1,2
10,0	5,7±0,1	6,0±2,0	8,0±2,0	7,0±2,0
12,5	6,5±0,2	6,4±1,1	8,3±1,3	7,9±0,9
15,0	6,7±0,2	6,9±2,3	9,5±1,7	8,3±0,7
20,0	–	3,0±0,8	13,0±5,8	11,0±2,8
25,0	10,7±0,4	5,5±1,1	8,9±3,0	9,6±2,2
PVA membrane	6,4±0,2	5,0±1,0	7,0±2,0	7,0±2,0

Table 5. Crystallite size for PVA crystalline phase at composite PVA/TiO₂ membranes.

100x	T _g (°C)	Water release		Melting			
		T _w (°C)	ΔH _w (J/g)	T _{m1} (°C)	ΔH _{m1} (J/g)	T _{m2} (°C)	ΔH _{m2} (J/g)
2,5	25,10	135,10	67,10	–	–	222,71	35,25
5,0	21,01	–	–	176,15	34,19	220,59	33,99
7,5	38,77	112,67	105,00	–	–	224,52	58,96
10,0	22,43	146,29	81,15	–	–	222,77	46,86
12,5	38,25	143,93	67,02	–	–	221,00	42,74
15,0	43,93	125,59	68,87	–	–	221,17	42,22
20,0	32,61	158,44	34,98	–	–	221,23	35,77
25,0	33,79	151,04	12,45	187,95	9,87	218,59	23,05
PVA membrane	22,38	–	–	ΔH = 169,5 J/g, T _m = 217,12			

Table 6. Important thermal parameters for PVA: TiO₂ composites, according to DSC thermograms.Figure 6. DSC thermograms of PVA: TiO₂ composite membranes, x equal to: (a) 0 (PVA), (b) 0,025, (c) 0,100, (d) 0,125 and (e) 0,250.

Results of XRD measurements confirm that water and ceramic fillers destroy crystallinity in PVA for small x values (100x<7,5). However, it is necessary taking into account the water molecules and the formation of intermediate regions which are larger than usual amorphous and crystalline phases [5,17]. Figure.6 indicates that TiO₂ fillers expand the free space at matrix and diminish the amount of superficial water bounded to PVA, allowing to strongly-bounded water molecules penetrating the interface between crystalline and amorphous phases, due to change of structural conformation at polymer chains, generating the crystallites destruction at polymeric matrix extending the short-range ordered regions (intermediate

states at amorphous phases), and improving the quality at remaining crystallites [17,26,39].

The rapprochement of macromolecular glass transition (T_g) at room temperature (22°C) shows that water molecules are almost entirely strongly bounded to polymer chains [21]. The endothermic phase transition associated to water molecules released (between 70 and 90°C) is influenced by thermal history and dried process on composite polymeric films, producing likewise recrystallization and reorientation of polymeric matrix, and starting from this temperature interval [22,26]. Therefore, liberation of superficial and strongly bounded water molecules, structural reordering and β-transition of crystalline phases at polymeric matrix are the responsible to produce melting of crystalline and intermediate phases into two steps: one of them between approx. 143 and 200°C [23,24] and other around 210°C, corresponding the last one to melting temperature of fully hydrolyzed PVA (T_m) [23,24,38,39].

D. Thermo-gravimetric Analysis (TGA)

Figure 7 show TGA and differential thermo-gravimetric analysis (DTG) thermograms of PVA: TiO₂ polymeric membranes. TGA and DTG curves reveal three weight loss regions, which appear as four peaks at DTG curves. The first region around 70-160°C is due to evaporation of physical (weakly) and chemical (strongly non-freezable) bounded water, the weight loss at membranes variates between 5,3 (100x = 25,0) and 8,3 % (PVA polymeric film) [27,40]. This weight loss region is correlated with endothermal width peak observed at DSC curve (Figure 6) [27]. The second region of weight loss around 220-360°C is due to melting and degradation of PVA: TiO₂ composite membranes, corresponding total weight loss is

located between 52,0 (100x = 25,0) and 79,7% (100x = 2,5), at PVA polymeric membrane the weight loss was 71,3% [27,40]. According to DSC results, in this second region the melting temperature of polymer is observed, like so an endothermic with a prominent enthalpy change associated to thermal degradation (Figure 6). DTG curves show two temperatures associated with maximal rates of weight loss (Figure 7) [27]. The third region between 360 and 500°C is due to breaking of PVA chains at membranes, the weight loss in this part variates between 8,0 and 17,3% [40]. Table 7 shows weight loss associated with regions mentioned above for PVA: TiO₂ composite membranes, for different x values.

Generally, the decomposition peaks of PVA: TiO₂ composite membranes exhibit a systematic evolution with an augment of 100x values. In fact, the second peak associated to melting and thermal degradation of PVA around 350°C shows a decrease at width and a more pronounced height, at direction in that 100x value augments. This point is an indicator of existing thermal correlation between crystalline order of TiO₂ ceramic fillers (confirmed from XRD results) and thermal decomposition of

PVA. The heating transfer through more ordered crystalline structure of TiO₂ to amorphous polymeric matrix of PVA augments the degradation rate associated with polymeric chains, which is centered more closely at 350°C. Evolution of peak associated to water liberation shows a similar behavior to degradation. However, augmenting 100x values, the intensity of peak around 430°C diminishes and the width augments, indicating a decrease at rate associated to breaking of PVA chains.

100x	First Region	Second Region	Third Region
0 (PVA polymer film)	8,353	71,32	17,36
2,5	6,634	79,72	8,970
5,0	7,279	71,07	16,36
7,5	7,496	70,48	8,066
10,0	6,926	72,26	13,92
12,5	6,964	64,57	16,12
15,0	7,300	68,60	16,36
20,0	6,351	56,46	13,55
25,0	5,335	52,02	8,176

Table 7. Weight loss at PVA: TiO₂ composite membranes.

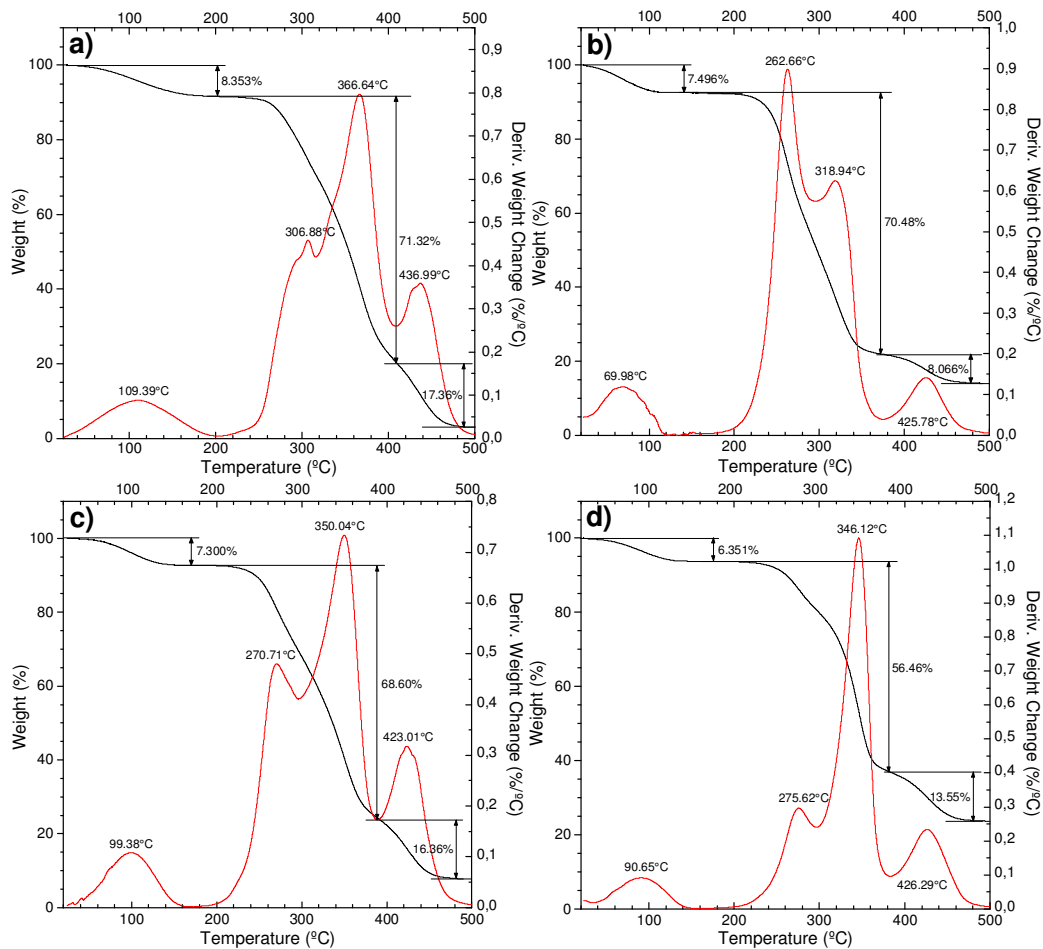


Figure 7. TG and DTG curves for PVA: TiO₂ polymeric membranes associated with different 100x values; (a) 0, (b) 7,5, (c) 15 and (d) 20.

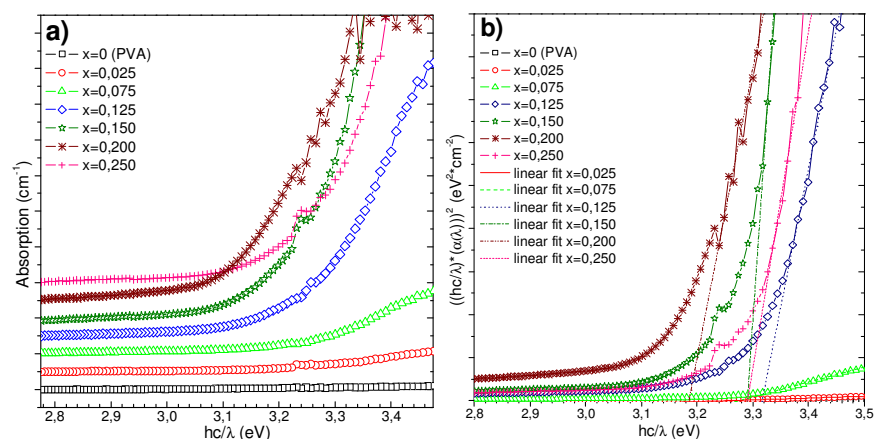


Figure 8. UV-visible absorption spectra for PVA: TiO₂ polymeric membranes; (a) absorption (cm⁻¹) and (b) Determination of E_g (allowed direct transitions DA) associated with TiO₂ (anatase).

100x	$\alpha(v)$ vs. (hc/λ)		$(\alpha(v))^2$ vs. (hc/λ)	
	¹ IA (eV)	¹ DA (eV)	¹ IA (eV)	¹ DA (eV)
2,5	2,983±0,006	3,200±0,005	2,995±0,006	3,268±0,002
7,5	3,029±0,007	3,223±0,003	3,031±0,007	3,282±0,002
12,5	3,038±0,005	3,251±0,003	3,071±0,004	3,313±0,003
15,0	3,045±0,004	3,246±0,005	3,083±0,005	3,278±0,005
20,0	2,969±0,006	3,250±0,005	3,077±0,005	3,299±0,005
25,0	2,946±0,006	3,162±0,009	3,019±0,005	3,211±0,010

Table 8. Calculated values for intrinsic transitions of TiO₂ (anatase).

E. UV-visible Absorption (UV-vis):

Figure 8 shows UV-vis absorption spectra for PVA: TiO₂ polymeric membranes. The composite processing conditions affect the energy bands and optical parameters [41]. The values of band gap are determined from curve absorption $\alpha(v)$ vs. incident photon energy (hc/λ) for PVA: TiO₂ composites spectra at UV-vis region. The absorption coefficient can be calculated from relation $\alpha(v) = \frac{A}{d}$; d is the sample thickness and A the absorbance. Calculated values of $\alpha(v)$ variates from 25 cm⁻¹ (PVA polymer film), 50 and 100 cm⁻¹ (100x = 2,5 and 7,5 respectively) to 800 cm⁻¹ for the others x values. These values may be attributed to changes at available final states number depending of blend composition, due to variations at structural conformation for semi-crystalline material [17,41].

Many regions and characteristic tendencies are observed near to UV absorption gap (2,8-3,4 eV for TiO₂, anatase) (Figure 8(b)). The energy values around 3,0-3,2 and 3,2-3,3 eV are characterized by the change at slope of tangent line at absorption curve. These characteristics can be associated with fundamental absorption (or intrinsic) of TiO₂ anatase. Then the values around 3,0-3,2 eV can be assigned to allowed indirect transitions from the edge to center of Brillouin zone. The characteristics around 3,2-3,3 eV can be assigned to allowed direct transitions. A gap of exponential absorption is also observed for $hc/\lambda > 3,0$ eV approximately [42].

Exponential dependence of absorption coefficient $\alpha(v)$ with photon energy (hc/λ) near to optical gap for some amorphous

and crystalline materials are given by equation proposed by Urbach, $\alpha(E) = \alpha_0 \exp \left[-\sigma \frac{E_0 - E}{k_B T} \right]$; E is photon energy, $\alpha(E)$ absorption coefficient, E_0 is an optical gap estimative, α_0 is a constant and σ is the strength parameter [17,43]. The extrapolation of linear portions at curve $(\alpha(v))^2$ vs. (hc/λ) (Figure 8(b)) has been calculated in order to find approximated values for TiO₂ (anatase) intrinsic transitions. The calculation of $(\alpha(v))^2$ vs. (hc/λ) curve is connected with direct absorption gap (E_g) by Tauc relation $\left(\alpha(v) * \frac{hc}{\lambda} \right)^2 = C \left(\frac{hc}{\lambda} - E_g \right)$ [43]. Table 8 shows calculated values for TiO₂ (anatase) intrinsic transitions at composite polymeric membranes. It can be seen that E_g values for PVA: TiO₂ blends show a slight shift compared with value for bulk TiO₂ (3,2 eV for anatase phase [6,44]). The fact above could reflect the induced changes at available final states number, considering tail band states, due to more disordered fillers, and the presence of crystalline, intermediate and amorphous regions at PVA polymeric matrix.

F. Scanning Electronic Microscopy (SEM)

SEM micrographs exhibiting the superficial morphology for PVA: TiO₂ composite membranes are shown at Figure 9 for different magnifications. The superficial morphology of composites shows randomly distributed chunks on surface. It has been seen that dimension of these TiO₂ chunks incorporated at PVA matrix is located around 2-5 μm . This fact indicates that ceramic fillers make aggregates and they are dispersed in PVA polymeric matrix [9]. However, in its whole, the compatibility of polymeric hydrophilic matrix of PVA and TiO₂ fillers has

demonstrated be homogeneous and compatible and not occurring separation at phases even taking into account the available quantity of ceramic filler incorporated to composites ($0,025 \leq x \leq 0,250$) [9,40].

IV. CONCLUSIONS:

PVA: TiO₂ composite membranes were sintered with good compatibility between the polymeric hydrophilic matrix of PVA and TiO₂ (anatase) fillers. The differences at contributions of amorphous and crystalline phases to different characterization measures were determined; these differences can be explicated thanks to steric effects present at structural conformation of polymer chain, due to presence of both, water molecules and TiO₂ ceramic fillers. Characteristic changes in function of temperature presented at molecular orientation of polymeric matrix were detected. Finally, three structural regions (crystalline, intermediate and amorphous) at PVA have been detected, and a polycrystalline and more disordered growing of TiO₂ particles in the PVA polymeric matrix has been found.

ACKNOWLEDGEMENTS:

The author wishes to acknowledge the academic advice provided by the Doctor J.F. Jurado. It is necessary to thanks to laboratories of: Química, Materiales Nano-Estructurados y Funcionales, Magnetismo y Materiales Avanzados, Física del Plasma and Propiedades Ópticas de los Materiales at National University of Colombia, Manizales. The same author also thanks to University of Texas at San Antonio (UTSA) by SEM micrographs. Finally, acknowledgements will be shown to Departamento Administrativo de Ciencia, Tecnología e Innovación-COLCIENCIAS by the opportunity provided through Convocatoria 566 de 2012 for young researchers.

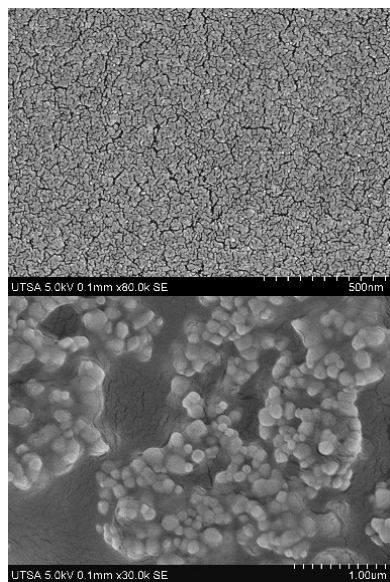


Figure 9. SEM micrographs for PVA/TiO₂ polymeric films at different magnifications.

REFERENCES:

- [1]. Raju, C. L., Rao, J.L., Reddy, B.C.V., Brahmam K. V., "Thermal and IR studies on copper doped polyvinyl alcohol" *Mater. Sci.* 30, 2007, 215–218.
- [2]. Abdelrazek E.M., El Damrawi G., Al-Shahawy A., "Some studies on calcium phosphate embedded in polyvinyl alcohol matrix before and after γ -irradiation" *Physica B.* 405(3), 2010, 808–816.
- [3]. Mishra R., Rao K.J., "On the formation of poly(ethyleneoxide)-poly(vinylalcohol) blends" *European Polymer Journal.* 35(10), 1999, 1883–1894.
- [4]. Sun P., Chen J., Liu Z.W., Liu Z.T., "Poly(vinyl alcohol) Functionalized β -Cyclodextrin as an Inclusion Complex" *Journal of Macromolecular Science, Part A: Pure and Applied Chemistry.* 46, 2009, 533–540.
- [5]. Kim D.S., Park H.B., Rhim J.W., Lee Y.M., "Preparation and characterization of crosslinked PVA/SiO₂ hybrid membranes containing sulfonic acid groups for direct methanol fuel cell applications" *Journal of Membrane Science.* 240(1–2), 2004, 37–48.
- [6]. Thamaphat K., Limsuwan P., Ngotawornchai B., Kasetsart J., "Phase Characterization of TiO₂ Powder by XRD and TEM" (*Nat. Sci.*), 42, 2008, 357–361.
- [7]. Mahdjoub N., Allen N., Kelly P., Vishnyakov V., "SEM and Raman study of thermally treated TiO₂ anatase nanopowders: Influence of calcination on photocatalytic activity" *Journal of Photochemistry and Photobiology A: Chemistry,* 211(1), 2010, 59–64.
- [8]. Lei P., Wang F., Gao X., Ding Y., Zhang S., Zhao J., Yang, M., "Immobilization of TiO₂ nanoparticles in polymeric substrates by chemical bonding for multi-cycle photodegradation of organic pollutants" *Journal of Hazardous Materials,* 227–228, 2012, 185–194.
- [9]. Yang C.C., Chiu S.J., Lee K.T., Chien W.C., Lin, C.T., Huang, C. A., "Study of poly(vinyl alcohol)/titanium oxide composite polymer membranes and their application on alkaline direct alcohol fuel cell" *Journal of Power Sources,* 184(1), 2008, 44–51.
- [10]. Wu Q., Zhang J., Sang S., "Preparation of alkaline solid polymer electrolyte based on PVA-TiO₂-KOH-H₂O and its performance in Zn-Ni battery" *Journal of Physics and Chemistry of Solids,* 69(11), 2008, 2691–2695.
- [11]. Yang C.C., Chien W.C., Li Y.J., "Direct methanol fuel cell based on poly(vinyl alcohol)/titanium oxide nanotubes/poly(styrene sulfonic acid) (PVA/nt-TiO₂/PSSA) composite polymer membrane" *Journal of Power Sources,* 195(11), 2010, 3407–3415.
- [12]. Toby B.H., "EXPGUI, a graphical user interface for GSAS" *J. Appl. Cryst,* 34, 2001, 210–213.
- [13]. Wojdyr M., "Fityk: a general-purpose peak fitting program" *J. Appl. Cryst,* 43, 2010, 1126–1128.
- [14]. Costa H.S., Rocha M.F., Andrade G.I., Barbosa-Stancioli E.F., Pereira M.M., Orefice R.L., Vasconcelos W.L., Mansur, H. S., "Sol-gel derived composite from bioactive glass-polyvinyl alcohol" *J. Mater. Sci.* 43, 2008, 494–502.

- [15]. Abdelrazek E.M., Elashmawi I.S., Labeeb S., "Chitosan filler effects on the experimental characterization, spectroscopic investigation and thermal studies of PVA/PVP blend films" *Physica B*, 405(8), 2010, 2021–2027.
- [16]. Socrates George, *Infrared and Raman Characteristic Group Frequencies Tables and Charts*, New York: Wiley, 2001, p. 50.
- [17]. Shehap A. M., "Thermal and spectroscopic studies of polyvinyl alcohol/sodium carboxy methyl cellulose blends" *Egypt. J. Solids*. 31(1), 2008, 75–91.
- [18]. Bhat N.V., Nate M.M., Kurup M.B., Bambole V. A., Sabharwal S., "Effect of γ -radiation on the structure and morphology of polyvinyl alcohol films" *Nuclear Instruments and Methods in Physics Research: Beam Interactions with Materials & Atoms*, 237, 2005, 585–592.
- [19]. Ma W., Lu Z., Zhang M., "Investigation of structural transformations in nanophase titanium dioxide by Raman spectroscopy" *Appl. Phys. A*, 66, 1998, 621–627.
- [20]. Radoičić M.B., Šaponjić Z.V., Marinović-Cincović M.T., Ahrenkiel S.P., Bibić N.M., Nedeljković J.M., "The influence of shaped TiO₂ nanofillers on thermal properties of polyvinyl alcohol" *Serb. Chem. Soc.*, 77(5), 2012, 699–714.
- [21]. Rault J., Gref R., Ping Z.H., Nguyen Q.T., Néel J., "Glass transition temperature regulation effect in a poly(vinyl alcohol)—water system" *Polymer*. 36(8), 1995, 1655–1661.
- [22]. Fonseca C., Pereña J.M., Benavente R., Cerrada M.L., Bello A., Pérez E. "Microhardness and thermal study of the annealing effects in vinyl alcohol—ethylene copolymers" *Polymer*. 36(9), 1995, 1887–1892.
- [23]. Fathi E., Atyabi N., Imani M. and Alinejad Z., "Physically crosslinked polyvinyl alcohol—dextran blend xerogels: Morphology and thermal behavior" *Carbohydrate Polymers*, 84(1), 2011, 145–152.
- [24]. Nugent M.J., Higginbotham C.L., "Investigation of the influence of freeze-thaw processing on the properties of polyvinyl alcohol/polyacrylic acid complexes" *J. Mater. Sci.*, 41, 2006, 2393–2404.
- [25]. Assender H.E., Windle A.H., "Crystallinity in poly(vinyl alcohol). 1. An X-ray diffraction study of atactic PVOH" *Polymer*, 39(18), 1998, 4295–4302.
- [26]. Zhang W., Zhang Z., Wang X., "Investigation on surface molecular conformations and pervaporation performance of the poly(vinyl alcohol) (PVA) membrane" *Journal of Colloid and Interface Science*, 333(1), 2009, 346–353.
- [27]. Jurado J.F., Checa O., Vargas R.A., "Investigation on the structure-electrical property relationship of hydrolyzed poly(vinyl alcohol) membranes" *Revista Mexicana de Física*, 59, 2013, 426–432.
- [28]. Bunn C.W. "Crystal Structure of Polyvinyl Alcohol" *Nature*, 161, 1948, 929–930.
- [29]. Cho J. D., Lyoo W. S., Chvalun S. N., Blackwell J., "X-ray analysis and molecular modeling of poly(vinyl alcohol)s with different stereoregularities" *Macromolecules*, 32 (19), 1999, 6236–6241.
- [30]. Shao Y., Tang D., Sun J., Lee Y., Xiong W., "Lattice deformation and phase transformation from nano-scale anatase to nano-scale rutile TiO₂ prepared by a sol-gel technique" *China Particuology*, 2(3), 2004, 119–123.
- [31]. Bokhimi X., Morales A., Aguilar M., Toledo-Antonio J.A., Pedraza F., "Local order in titania polymorphs" *Int. J. Hydrogen Energ.*, 26(12), 2001, 1279–1287.
- [32]. Minus M.L., Chae H.G., Kumar S., "Single wall carbon nanotube templated oriented crystallization of poly(vinyl alcohol)" *Polymer*, 47 (11), 2006, 3705–3710.
- [33]. Lee Y.M., Kim S.H., Kim S.J., "Preparation and characteristics of β -chitin and poly(vinyl alcohol) blend" *Polymer*, 37(26), 1996, 5897–5905.
- [34]. Assender H.E., Windle A.H., "Crystallinity in poly(vinyl alcohol). 2. Computer modelling of crystal structure over a range of tacticities" *Polymer*, 39(18), 1998, 4303–4312.
- [35]. JCPDS cards: No 21–1272 and No 71–1169.
- [36]. Cerrada M.L., Pérez E., Pereña J.M., Benavente R., "Wide-Angle X-ray Diffraction Study of the Phase Behavior of Vinyl Alcohol—Ethylene Copolymers" *Macromolecules*, 31, 1998, 2559–2564.
- [37]. Khanna P.K., Singh N., Charan S., "Synthesis of nanoparticles of anatase-TiO₂ and preparation of its optically transparent film in PVA" *Materials Letters*. 61, 2007, 4725–4730.
- [38]. Wiria F.E., Chua C.K., Leong K.F., Quah Z.Y., Chandrasekaran M., Lee M.W., "Improved biocomposite development of poly(vinyl alcohol) and hydroxyapatite for tissue engineering scaffold fabrication using selective laser sintering" *J. Mater. Sci.: Mater. Med*, 19, 2008, 989–996.
- [39]. Hodge R.M., Edward G.H., Simon G.P., "Water absorption and states of water in semicrystalline poly(vinyl alcohol) films" *Polymer*, 37(8), 1996, 1371–1376.
- [40]. Yang C.C., "Synthesis and characterization of the cross-linked PVA/TiO₂ composite polymer membrane for alkaline DMFC" *Journal of Membrane Science*, 288, 2007, 51–60.
- [41]. El-Sayed S., Mahmoud K.H., Fatah A.A., Hassen A., "DSC, TGA and dielectric properties of carboxymethyl cellulose/polyvinyl alcohol blends" *Physica B*, 406(21), 2011, 4068–4076.
- [42]. Kernazhitsky L., Shymanovska V., Gavrillo T., Naumov V., Fedorenko L., Kshnyakin V., Baran J., "Room temperature photoluminescence of anatase and rutile TiO₂ powders" *Journal of Luminescence*. 146, 2014, 199–204.
- [43]. Tauc J. (Ed.), *Amorphous and Liquid Semiconductors*, New York: Plenum Press, 1974, p. 170–177.
- [44]. Xu T.H., Song C.L., Liu Y., Han G.R., "Band structures of TiO₂ doped with N, C and B" *J. Zhejiang Univ. SCIENCE B*, 7(4), 2006, 299–303.